RSC Advances

PAPER

View Article Online
View Journal | View Issue

Cite this: *RSC Adv.*, 2020, **10**, 11311

Determination of acid dissociation constants of Alizarin Red S, Methyl Orange, Bromothymol Blue and Bromophenol Blue using a digital camera†

Ahmed A. Shalaby and Ashraf A. Mohamed *

Received 16th December 2019
Accepted 13th March 2020

DOI: 10.1039/c9ra10568a

rsc.li/rsc-advances

Acid dissociation constants (pK_a) are important parameters for the characterization of organic and inorganic compounds. They play a crucial role in different physical, chemical, and biological studies. Herein, we introduce a new approach for the determination of acid dissociation constant based on digital image analysis using a low-cost, precise, accurate, sensitive, and portable home-made, camera-based platform. Digital images of Alizarin Red S, Bromophenol Blue, Bromothymol Blue, and Methyl Orange solutions were captured at various pH values. The captured images were analysed to obtain the RGB (Red, Green, and Blue) colour intensities that are used to calculate the RGB colour absorbances. The pK_a values were calculated from the RGB colour absorbance–pH relationship using graphical and mathematical methods, and with the aid of DATAN software. For the four studied dyes, the results obtained from digital image analysis were in excellent agreement with the data of sophisticated spectrophotometers and the previously reported literature data.

1. Introduction

Acid dissociation constants (pK_as) are important parameters in physical, chemical, and biochemical studies. They indicate the extents of ionization of the acidic groups in the molecules at various pH values. They play a basic role in different analytical procedures such as acid–base titrations, complex formations, and solvent extraction. Various methods were used to determine the pK_a values including spectrophotometry,[1–9] spectrofluorimetry,[10] potentiometry,[1,10–13] conductometry,[14,15] cyclic voltammetry,[16] chromatography,[1,17–20] electrophoresis,[21,22] NMR,[23,24] mass spectrometry,[25] and Raman spectroscopy;[26] however the majority of these methods require expensive and sophisticated instruments. Therefore, solution scanometric methods were used,[27–30] but the lack of uniformity of the captured images greatly affected the precision of the analysis posing a serious disadvantage of these methods.[27–30]

Recently, digital image-based analysis (DIBA) methods have been widely used for colorimetric analysis. These methods use digital cameras,[31–33] smartphone cameras,[32–36] or scanners,[32,33,37] as colorimetric sensors, where various colour spaces parameters were used as analytical signalling tools.[32,33] The RGB colour system is the most widely used colour space and its parameters value can be obtained directly from the images by various image analysis software, *e.g.*, Adobe Photoshop, and ImageJ.[32,33]

Herein we present a very simple, low-cost, accurate, sensitive, and precise digital camera-based approach for the determination of single and consecutive acid dissociation constants. The pK_a values of the diprotic Alizarin Red S (ARS), and the monoprotic Bromophenol Blue (BPB), Bromothymol Blue (BTB), and Methyl Orange (MO) dyes were determined as model examples. A conventional digital camera was used to capture digital images of dyes solutions adjusted to various pH values. Captured digital images were analysed to yield the Red, Green, and Blue (RGB) intensities that were used to calculate the RGB colour absorbances. The relation between the obtained RGB colour absorbances and the pH values were used to calculate the pK_a values using graphical and mathematical methods. Further, the pK_a values were calculated using DATAN software based on the RGB colour absorbance–pH relationship.[4,38–40] The results of DIBA method competed well with the results of the spectrophotometric method and the previously reported literatures data.

2. Experimental

2.1. Apparatus and software

Spectrophotometric measurements in 1 cm matched quartz cells in the range of 190–1100 nm were made on a Shimadzu (Kyoto, Japan) 1601 UV/VIS Spectrophotometer controlled by an UVProbe-2.5 software. Eppendorf 10–100 and 100–1000 μL varypipettes (Westbury, NY, USA) and a calibrated EDT pH–mV meter (Dover Kent, UK) were used.

Department of Chemistry, Faculty of Science, Ain Shams University, Abbassia, Cairo-11566, Egypt. E-mail: aamohamd@sci.asu.edu.eg; Fax: +202 24831836; Tel: +201001578849

† Electronic supplementary information (ESI) available. See DOI: 10.1039/c9ra10568a

Digital images were captured using a Canon PowerShot A810 digital camera that is equipped with a 16.0 Mega Pixel CCD sensor. DIBA measurements were made using a simple home-made platform (spectrometer)[32,33] that does not require any lens, slit, mirror, wavelength selector, or signal amplifier. It consisted of (1) two quartz cells (2) the digital camera as a detector and (3) a white paper as background diffuser; where, the diffuser, the cell-holder and camera-holder were fixed on a wood plate; each of them was 5 cm distance apart.[32,33] Digital images were captured in our laboratory, where the conventional fluorescent daylight-lamp fixed at the laboratory ceiling served as the light source.[32,33]

A conventional HP-Pavilion dv6-6176ex Notebook running under Windows 10 was used for data treatment and analysis. Photoshop CC 2016 and ImageJ software 1.52 were used for digital image processing and determination of RGB channel intensities. DATAN 5.0 software was used for pK_a calculations from both spectrophotometric and digital image processed data.[41]

2.2. Reagents and solutions

All reagents were of ACS grade and were used as received from Sigma-Aldrich (St. Louis, MO, USA), or Merck (Darmstadt, Germany). Unless otherwise stated, bi-distilled water and aqueous solutions were used throughout. The following stock indicator solutions were prepared: aqueous 3.0×10^{-4} mol L^{-1} Methyl Orange (MO), aqueous 3.0×10^{-4} mol L^{-1} Alizarine Red S (ARS), 20% ethanolic solution of 3.0×10^{-4} mol L^{-1} Bromophenol Blue (BPB), and ethanolic solution of 3.0×10^{-4} mol L^{-1} Bromothymol Blue (BTB).

For DIBA and spectrophotometric measurements, 5.0–20.0 mL aliquot of a stock indicator solution was diluted to 100 mL to give the following working indicator solutions: 3.0×10^{-5} mol L^{-1} MO, 6.0×10^{-5} mol L^{-1} ARS, 1% ethanolic solution of 1.5×10^{-5} mol L^{-1} BPB, and 20% ethanolic solution of 3.0×10^{-5} mol L^{-1} BTB.

2.3. Spectrophotometric and (DIBA) measurements

Each working indicator solution was successively treated with few microliters of 2.0 mol L^{-1} HCl or NaOH. After each addition, the pH was adjusted and portions of the well-stirred solution were transferred to the cells of both the spectrophotometer and our homemade spectrometer to record the absorption spectrum and capture digital images of the sample and blank cells, respectively. After each measurement, solutions were returned to the titration vessel. The final volume after each addition was recorded and then used to correct the values of the measured absorbance or RGB colour absorbance. A captured image was processed by Photoshop CC 2016 and ImageJ 1.52 software to crop an Area Of Interest (AOI: a square of 354×354 pixels where any predefined area can be used because the images are homogenous) and calculate the mean RGB channel intensities, I_R, I_G, I_B, respectively. An image RGB absorbance is calculated from RGB intensities of the sample and blank [$A_{RGB} = \log (I_o/I)$ = log((colour intensity of the blank)/(colour intensity of the sample))].[32,33] A_{RGB} values were then plotted against solution pH's yielding the characteristic sigmoid shaped titration curve.

2.4. pK_a calculations using DIBA and spectrophotometric data

2.4.1. Graphical determination of pK_a from titration curves. Absorbance (or RGB colour absorbance)–pH graphs were used to calculate the respective pK_a values where the pK_a value is represented by the pH at half the inflection of the sigmoid graph.[17,25,26,42] For a more accurate determination of pK_a the 2nd derivative graphs were also plotted.

2.4.2. Mathematical and graphical determination of pK_a from the mole fraction. For an acid $HA \leftrightarrow A^- + H^+$

The mole fractions are calculated using eqn (1) and (2)[43]

$$X_{A^-} = \frac{(A - A_{HA})}{(A_{A^-} - A_{HA})} \quad (1)$$

$$X_{HA} = 1 - X_{A^-} \quad (2)$$

The mole fraction is plotted against the pH values and the pK_a is equal to the pH at the intersection between the mole fraction lines where $X_{A^-} = X_{HA} = 0.5$.

Further, the pK_a was determined using eqn (3)[43]

$$pH = pK_a + \log \frac{(A - A_{HA})}{(A_{A^-} - A)} \quad (3)$$

where A is the absorbance at any pH value and A_{A^-} and A_{HA} are the absorbance values of the pure ionized and protonated forms, respectively.

2.4.3. Calculation of pK_a using the DATAN 5.0 software. For calculation of pK_a using DATAN program, the absorption spectra and the RGB absorption data of each indicator at various pH values were loaded into DATAN 5.0 in the form of excel worksheet, and then subjected to principal component analysis (PCA) to confirm the number of chemical species present during the pH-metric titration, and then subjected to protolytic analysis depending on the number of species produced to calculate the pK_a values.

3. Results and discussion

3.1. Graphical determination of pK_a's from titration data

For determination of the pK_a values the absorption spectra at various pH values for the four dyes used were recorded in the wavelength range 230–700 nm as given in Fig. 1. The absorbance values at peak maxima were used in the pK_a determination. For ARS, the absorbance–pH graphs at the wavelengths of maximum absorptions of 333.5, 420, 517, 556 and 593 nm along with their 2nd derivative counterparts are shown in Fig. 2A and B. ARS have two ionizable protons so two inflections appear in some titration curves. From the second derivative graphs, the pK_a of the first ionization is 5.82, 5.84, 5.82, 5.82, and 5.82 at the selected wavelengths, respectively with an average of 5.82; while the pK_a for the second ionization appeared only at 333.5 nm, 556 nm, and 593 nm with values 10.55, 10.90, and 10.88, respectively with an average of 10.78.

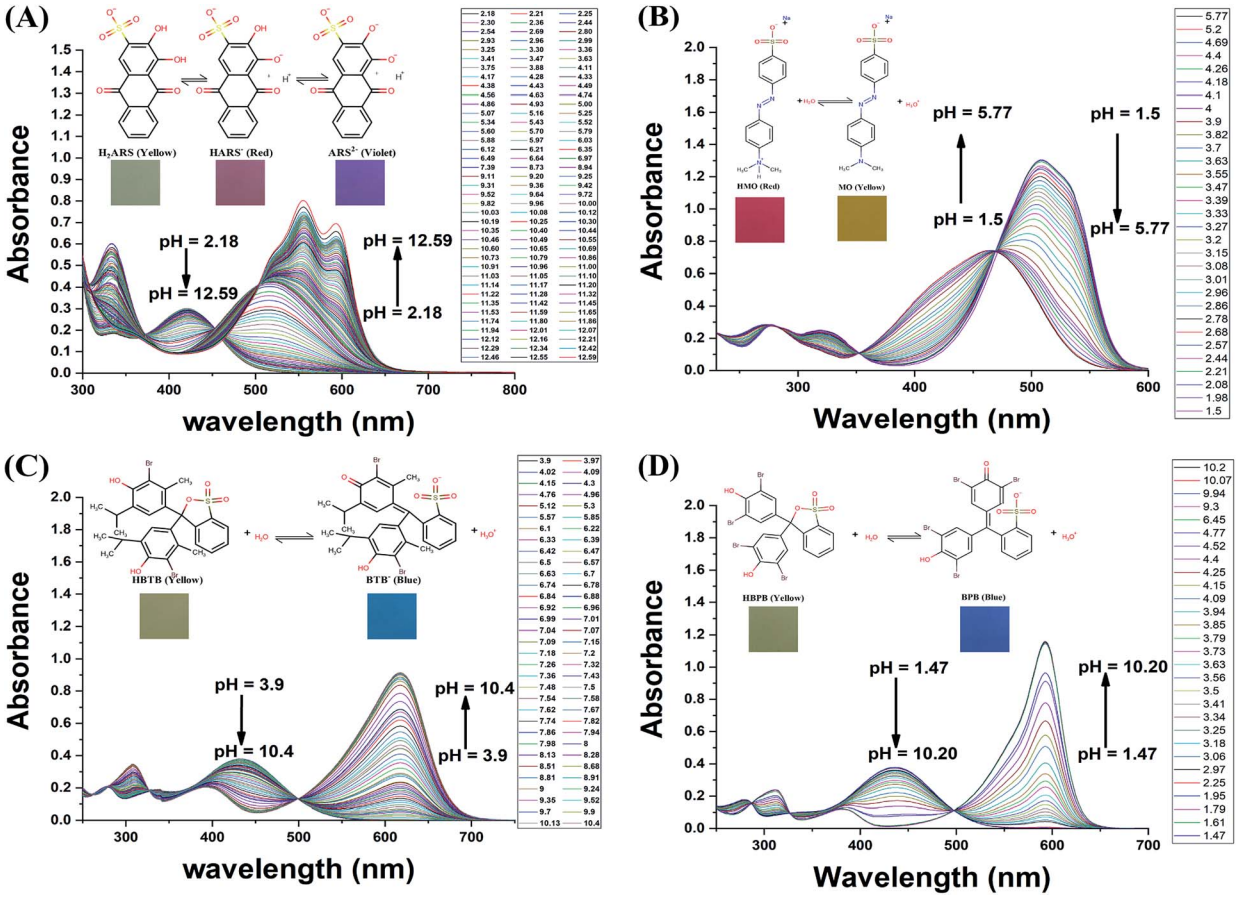

Fig. 1 The absorption spectra in range 230–700 nm for the dyes used at different pH values (A) Alizarin Red S, (B) Methyl Orange, (C) Bromothymol Blue, and (D) Bromophenol Blue. Each graph contains the structure of the ionized and nonionized forms and the digital image each form.

The digital images at various pH values for ARS and Cropped Area Of Interest (AOI) are shown in Fig. S1 and S2,† the colour changes from yellow (H_2ARS) to red ($HARS^-$) around the first ionization and from red ($HARS^-$) to violet (ARS^{2-}) around the second ionization. The RGB colour absorbance–pH relation for the RGB channels exhibited two inflections on the sigmoidal curve for both the red and blue Channels while exhibiting one inflection only for the green channel, this is due to the colour change from red to the violet around the second ionization where the change in the green channel absorbance will be gradual with the pH change as shown Fig. 2C. From the corresponding second derivative plot in Fig. 2D, the first pK_a is 5.50, 5.89, and 6.17 for red, green and blue respectively with average 5.85 while the second pK_a is 10.73 and 10.84 for red and blue respectively with average 10.78.

Similarly, the digital images and the cropped AOI for MO, BTB, and BPB are shown in Fig. S3–S8.† Each one of the three dyes has only one pK_a with colour change from red to yellow for MO and from yellow to blue for BTB and BPB. Fig. S9† shows titration curves and the 2nd derivative graphs for the three dyes with DIBA and spectrophotometrically. The RGB data gave pK_a values of 3.64, 3.67, and 3.36 for MO, 4.27, 4.26, and 3.94 for BPB, and 7.74, 7.45, and 7.48 for BTB for the red, green, and blue channels, respectively. While, the spectrophotometric data gave pK_a values for MO 3.52, 3.58, and 3.57 at 319 nm, 464 nm, and 508 nm, respectively; while for BPB gave 4.14, 4.17, and 4.15 at 311 nm, 436 nm, and 593 nm, respectively; and for BTB gave 7.48, 7.55, and 7.52 at 307 nm, 433 nm, and 617 nm, respectively.

Table 1 shows the average pK_a values obtained for the four dyes used at various wavelengths and RGB colour channels. The statistical t-test indicates that at 95% confidence level there is no significant difference between the means obtained from the two methods ($t_{calculated} < t_{tabulated}$ & $p > 0.05$). Also, the paired t-test gave p value = 0.116 and $|t| = 2.000 < t_{table} = 2.306$ and this is confirming that no significant difference can be detected between the means obtained. Fig. 2E shows a correlation between the pK_a values obtained from the two techniques; the 95% confidence intervals of the slope is 0.9888–1.0116 therefore the slope is not significantly different from 1.0000. Similarly, the 95% confidence interval of the intercept is −0.0642–0.0934 therefore the intercept is not significantly different from 0.00, this confirm the excellent agreement between the pK_a values obtained from the DIBA and the spectrophotometry.

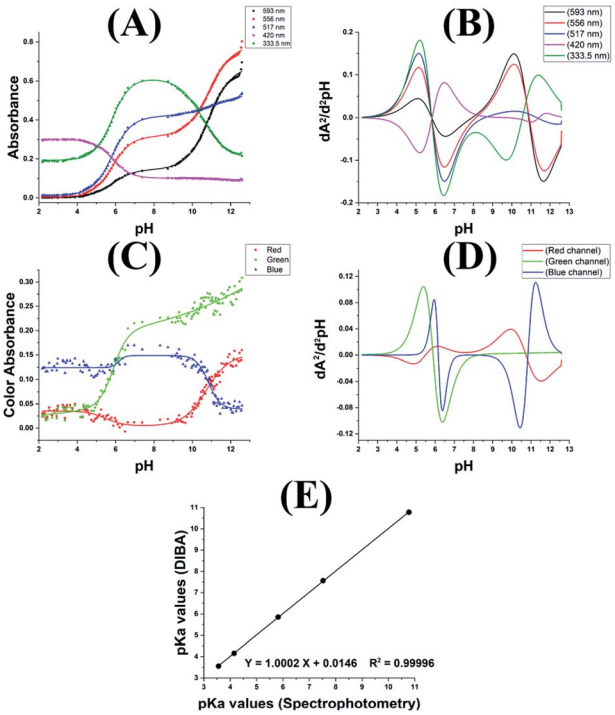

Fig. 2 Absorbance–pH relation (A) and its 2nd derivative plot (B), RGB colour absorbance–pH relation (C) and its 2nd derivative plot (D) for Alizarin Red S. (E) RGB correlation graph between the pK_a values obtained by DIBA and spectrophotometry for the four dyes used.

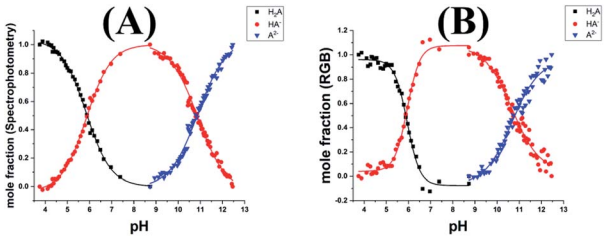

Fig. 3 The distribution of the pure species of the Alizarin Red S as a function of pH using spectrophotometry (A) and DIBA (B).

3.2. Graphical and mathematical determination of pK_a values using mole fraction calculations

To calculate the mole fraction of each species, firstly we choose the spectra and the RGB values corresponding to the pure species. For the studied dyes, the fully protonated forms and the fully deprotonated forms were chosen at the lowest and the highest pH values, respectively. While for ARS the spectra and the RGB values of the pure mono protonated form ($HARS^-$) was chosen at the pH 8.73. After that the mole fraction was calculated at each pH value using eqn (1) and (2). Fig. 3A and B shows the relation between the pH of ARS solutions and the mole fractions calculated spectrophotometrically and from the RGB data, respectively. Similarly, Fig. S10† shows the mole fraction graphs for MO, BTB, and BPB. The pK_a values obtained by DIBA and spectrophotometrically were given in Table 2. At the 95% confidence level, the paired *t*-test gave *t*-value 1.90 and *p* value 0.130 indicating that there is no significant difference between the values obtained from the two techniques.

Moreover, the protonated and deprotonated species were considered as a mixture of a weak acid and its salt so that the pK_a can be calculated mathematically using eqn (3). The pK_a values obtained were presented in Table 2. Similarly, at the 95% confidence level, the paired *t*-test gave *t*-value of 2.13 and *p* value of 0.100, indicating that there is no significant difference between the two techniques.

3.3. Calculation of pK_a values using the DATAN 5.0 software

The pK_a values of the four studied dyes used were determined by DATAN 5.0 program using the RGB and the spectrophotometric data. The PCA analysis of both the RGB and spectrophotometric data confirm the presence of three species (H_2A, HA^-, and A^{2-}) for ARS and two species (HA and A^-) for MO, BPB, and BTB during the pH metric titration. The protolytic analysis of ARS using the RGB and spectrophotometric data outputted (1) the calculated pure spectra of various species present, Fig. 4A and B, (2) the molar ratio plot showing calculated distribution diagram of various species, Fig. 4C and D and (3) the pK_a values as the pH values at the intersections of the molar ratio lines of different species, Table 2. Similarly, the protolytic analysis of MO, BPB, and BTB data were presented in Fig. S11† and Table 2. At the 95% confidence level the paired *t*-test gave *t*-value of 1.27 and *p*

Table 1 pK_a values obtained graphically from the relation between pH and absorbance or RGB colour absorbance[a]

Indicator		Spectrophotometry	DIBA	$\lvert t_{0.05}\ (3,3)\rvert$ $t_{table} = 2.776$	*p* value $P_{table} = 0.05$
ARS	pK_{a1}	5.82 ± 0.01	5.85 ± 0.34	0.151*	0.894
	pK_{a2}	10.78 ± 0.2	10.78 ± 0.08	0.066**	0.953
BPB		4.15 ± 0.02	4.16 ± 0.19	0.031	0.978
BTB		7.52 ± 0.04	7.56 ± 0.16	0.424	0.713
MO		3.56 ± 0.03	3.56 ± 0.17	0.000	1.000

[a] *$t_{0.05}$ (5,3), $t_{table} = 2.447$, **$t_{0.05}$ (3,2), $t_{table} = 3.182$.

Table 2 The pK_a values obtained from DIBA and spectrophotometry using the different methods

		Experimental values						
		Mole fraction		Mathematically[a]		DATAN		
		RGB	Spectrophotometry	RGB	Spectrophotometry	RGB	Spectrophotometry	Literature value [from ref. 44]
ARS	pK_{a1}	5.88	5.86	5.72	5.70	5.96	5.80	5.49
	pK_{a2}	10.81	10.86	10.78	10.73	10.72	10.74	10.85
BPB		4.14	4.17	4.21	4.21	4.20	4.16	4.10
BTB		7.60	7.64	7.62	7.50	7.72	7.52	7.30
MO		3.47	3.60	3.55	3.52	3.51	3.57	3.46

[a] Using eqn (3).

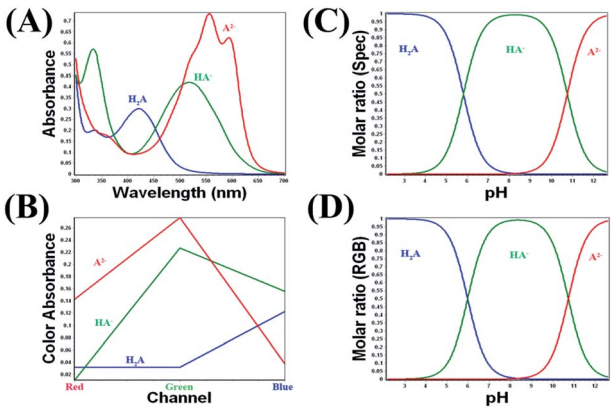

Fig. 4 The pure spectra (A) and the pure RGB absorbance values (B) of the different species of Alizarin Red S. The distribution plot of Alizarin Red S pure species using spectrophotometry (C) and RGB absorbance values (D).

value of 0.273 indicating that there is no significant difference between the two techniques.

4. Conclusion

In this work we introduce a new approach for the determination of acid dissociation constant (pK_a) based on digital image analysis using low-cost, accurate, and precise camera-based home-made platform. The pK_a values of four different organic dyes were determined. Alizarin Red S was used as example for molecules having two consecutive pK_a values; while Bromophenol Blue, Bromothymol Blue, and Methyl Orange were used as examples for molecules with single pK_a value. The pK_a was determined using the RGB colour absorbance by five different methods for calculation distributed between graphically, mathematically, and using the DATAN program. The results obtained from the digital image analysis give excellent agreement with the results of the spectrophotometric methods and the previously reported literature's data in all of the studied cases, Tables 1 and 2. The time required for each measurement and its subsequent RGB data analysis can be double the time for sophisticated spectrophotometric measurements. However, the low-cost, accuracy, repeatability and affordability to most resource limited laboratories are added advantages of the current approach.

Conflicts of interest

There are no conflicts to declare.

Notes and references

1 M. B. Polat, A. Doğan and N. E. Başcı, *J. Res. Pharm.*, 2019, **23**, 177–186.
2 M. Meloun, L. Pilařová, A. Pfeiferová and T. Pekárek, *J. Solution Chem.*, 2019, **48**, 1266–1286.
3 N. Kapilraj, S. Keerthanan and M. Sithambaresan, *J. Chem.*, 2019, **2019**, 1–6.
4 A. Dadras, A. Benvidi, M. Namazian, S. Abbasi, D. Tezerjani, M. Roozegari and R. Tabaraki, *J. Serb. Chem. Soc.*, 2019, **84**, 391–403.
5 A. Benvidi, A. Dadras, S. Abbasi, M. D. Tezerjani, M. Rezaeinasab, R. Tabaraki and M. Namazian, *J. Chin. Chem. Soc.*, 2019, **66**, 589–593.
6 A. Zafra-Roldan, S. Corona-Avendano, R. Montes-Sanchez, M. Palomar-Pardave, M. Romero-Romo and M. T. Ramirez-Silva, *Spectrochim. Acta, Part A*, 2018, **190**, 442–449.
7 R. Romero, P. R. Salgado, C. Soto, D. Contreras and V. Melin, *Front. Chem.*, 2018, **6**, 208.
8 M. Meloun, L. Pilařová, A. Čápová and T. Pekárek, *J. Solution Chem.*, 2018, **47**, 806–826.
9 R. Hadjeb and D. Barkat, *Arabian J. Chem.*, 2017, **10**, S3646–S3651.
10 D. T. Taskiran, G. O. Urut, S. Ayata and S. Alp, *J. Fluoresc.*, 2017, **27**, 521–528.
11 V. Arunachalam, A. K. Tummanapelli and S. Vasudevan, *Phys. Chem. Chem. Phys.*, 2019, **21**, 9212–9217.
12 A. Soames, S. Iglauer, A. Barifcani and R. Gubner, *J. Chem. Eng. Data*, 2018, **63**, 2904–2913.
13 H. A. Zayas, A. McCluskey, M. C. Bowyer and C. I. Holdsworth, *Anal. Methods*, 2015, **7**, 8206–8211.
14 J. Reijenga, A. van Hoof, A. van Loon and B. Teunissen, *Anal. Chem. Insights*, 2013, **8**, 53–71.
15 M. Klučáková, *React. Funct. Polym.*, 2018, **128**, 24–28.

16 F. Zonouzi, A. Shayesteh, T. Alizadeh, H. Dezhampanah, B. Ghalami-Choobar and A. Zonouzi, *J. Chin. Chem. Soc.*, 2019, **67**(1), 41–45.
17 J. Savić, B. Marković, V. Vitnik and S. Dilber, *Kragujevac J. Sci.*, 2018, 103–111, DOI: 10.5937/KgJSci1840103S.
18 G. Rabah, *J. Chem. Educ.*, 2018, **95**, 310–314.
19 T. Volna, K. Motyka and J. Hlavac, *J. Pharm. Biomed. Anal.*, 2017, **134**, 143–148.
20 T. Angelov and I. Hristov, *J. Liq. Chromatogr. Relat. Technol.*, 2018, **41**, 87–92.
21 P. M. Nowak, M. Wozniakiewicz, M. Piwowarska and P. Koscielniak, *J. Chromatogr. A*, 2016, **1446**, 149–157.
22 S. K. Poole, S. Patel, K. Dehring, H. Workman and C. F. Poole, *J. Chromatogr. A*, 2004, **1037**, 445–454.
23 A. Mumcu and H. Kucukbay, *Magn. Reson. Chem.*, 2015, **53**, 1024–1030.
24 E. Parman, L. Toom, S. Selberg and I. Leito, *J. Phys. Org. Chem.*, 2019, **32**(6), e3940.
25 J. F. Feehan, J. Monaghan, C. G. Gill and E. T. Krogh, *Environ. Toxicol. Chem.*, 2019, **38**, 1879–1889.
26 B. H. Pogostin, A. Malmendal, C. H. Londergan and K. S. Akerfeldt, *Molecules*, 2019, **24**(3), 405.
27 A. Shokrollahi, M. Gohari and F. Ebrahimi, *Anal. Bioanal. Chem. Res.*, 2018, **5**, 67–79.
28 A. Shokrollahi and E. Zare, *J. Mol. Liq.*, 2016, **219**, 1165–1171.
29 A. Shokrollahi and F. Firoozbakht, *BJBAS*, 2016, **5**, 13–20.
30 A. Shokrollahi, F. Zarghampour, S. Akbari and A. Salehi, *Anal. Methods*, 2015, **7**, 3551–3558.
31 T. T. Wang, C. K. Lio, H. Huang, R. Y. Wang, H. Zhou, P. Luo and L. S. Qing, *Talanta*, 2020, **206**, 120211.
32 A. A. Mohamed and A. A. Shalaby, *Food Chem.*, 2019, **274**, 360–367.
33 A. A. Mohamed, A. A. Shalaby and A. M. Salem, *RSC Adv.*, 2018, **8**, 10673–10679.
34 J. Liu, Z. Geng, Z. Fan, J. Liu and H. Chen, *Biosens. Bioelectron.*, 2019, **132**, 17–37.
35 H. Wang, Y. Sun, H. Li, W. Yue, Q. Kang and D. Shen, *Sens. Actuators, B*, 2018, **271**, 358–366.
36 V. Kılıç, G. Alankus, N. Horzum, A. Y. Mutlu, A. Bayram and M. E. Solmaz, *ACS Omega*, 2018, **3**, 5531–5536.
37 B. Pang, C. Zhao, L. Li, X. Song, K. Xu, J. Wang, Y. Liu, K. Fu, H. Bao, D. Song, X. Meng, X. Qu, Z. Zhang and J. Li, *Anal. Biochem.*, 2018, **542**, 58–62.
38 T. Momeni-Isfahani and A. Niazi, *Spectrochim. Acta, Part A*, 2014, **120**, 630–635.
39 A. Niazi, M. Ghalie, A. Yazdanipour and J. Ghasemi, *Spectrochim. Acta, Part A*, 2006, **64**, 660–664.
40 J. Ghasemi, S. Lotfi, M. Safaeian, A. Niazi, M. M. Ardakani and M. Noroozi, *J. Chem. Eng. Data*, 2006, **51**, 1530–1535.
41 https://multid.se/DATAN/, accessed 30 June, 2019.
42 A. R. Ribeiro and T. C. Schmidt, *Chemosphere*, 2017, **169**, 524–533.
43 A. Albert and E. P. Serjeant, *The Determination of Ionization Constants*, CHAPMAN AND HAll, New York, USA, 3rd edn, 1984.
44 E. Bishop, *Indicators*, Pergamon Press, Oxford, 1972.